Effects of spin-orbit interaction in photoelectron scattering process for magnetic EXAFS

A. Koide, J. Kogo, K. Niki, D. Sébilleau

Effects of spin-orbit interaction in photoelectron scattering process for magnetic EXAFS

A. Koide[a,b], J. Kogo[c], K. Niki[c], D. Sébilleau[b]

[a] *Graduate School of Advanced Integration Science, Chiba University, 1-33 Yayoi-cho, Inage-ku, Chiba, 263-8522, Japan*
[b] *Univ Rennes, CNRS, IPR (Institut de Physique de Rennes) - UMR 6251, F-35000 Rennes, France*
[c] *Graduate School of Science and Engineering, Chiba University, 1-33 Yayoi-cho, Inage-ku, Chiba, 263-8522, Japan*

Abstract

We present an effect of the spin-orbit interaction (SOI) at surrounding atoms on K-edge magnetic extended x-ray absorption fine structure (MEXAFS). A contribution of the SOI to a K-edge MEXAFS spectrum is described by a perturbative way within a multiple scattering (MS) theory. A numerical calculation shows that a photoelectron single scattering by the SOI at surrounding atomic sites has a negligibly small contribution to MEXAFS. Although a negligible contribution of the SOI at surrounding atoms has been attributed to a cancellation of various MS contributions, this small contribution can be understood by the small number of its effective partial wave components, at least within the single scattering approximation. For further detailed analyses of MS with a path expansion method, only the small number of the partial wave components for the SOI is necessary. This leads to faster computations for MEXAFS including the photoelectron scattering by the SOI.

Keywords: MEXAFS, Multiple scattering theory, Spin orbit interaction

1. Introduction

Magnetic extended x-ray absorption fine structure (MEXAFS) is x-ray magnetic circular dichroism (XMCD) extended to the higher photon energy region and applied to magnetic materials to obtain the local spin-pair-distribution function [1]. The K-edge MEXAFS spectrum provides oscillated spectral structures in the wide energy range, which is effective for the pair-distribution function transformed from the MEXAFS oscillations by using a finite Fourier transformation [1]. To give rise to the intensity of XMCD or MEXAFS, the spin-orbit interaction (SOI) originating from a relativistic correction has to be taken account because it partially connects the helicity of the incident x-rays to the spin state of the excited core electron. In particular, the core 1s orbital, as the initial state in the K-edge absorption, has no orbital momentum and is not affected by the SOI. Hence, K-edge MEXAFS (as well as XMCD) requires the SOI acting on unoccupied p states within the dipole optical transition.

Although fully relativistic MEXAFS calculations have been reported [2], theoretical description of MEXAFS based on including the SOI as a perturbation is useful because it enables to take into account the the Debye-Waller factor [3, 4, 5, 6, 7, 8, 9]. Ankudinov et al. [3, 4] and Fujikawa et al. [5, 6] considered the SOI only at an absorbing atom in an intrinsic process within a multiple scattering (MS) theory where a photoelectron is not scattered by the SOI but only by each effective site potential. While Brouder et al. incorporated the SOI at all atomic sites in an extrinsic process where a photoelectron is scattered by the perturbative SOI and each effective site potential [7, 8, 9]. A calculation of K-edge MEXAFS showed that the contribution of the SOI in the extrinsic process can be neglected [9]. This negligible contribution was attributed to a cancellation of various MS contributions. However, the mechanism how this contribution gets small is still not clear because the calculation was performed by using full MS, which does not keep trace of each individual MS path contribution. A path-expansion analysis would be useful in order to deeply understand MS effects on MEXAFS, which could be rather different from what there are in the case of extended x-ray absorption fine structure (EXAFS) [10].

In Ref. 11, we have reported in detail effects of the SOI on K-edge XMCD (but not MEXAFS) [11]. It was found that a more precise expression of a single scattering term in the extrinsic process differs from a single scattering approximation of the full MS term which was used to show the cancellation. It is worth to perform a numerical check of the single scattering term as the first step of the path-expansion analysis for the extrinsic process.

In this work, we perform K-edge MEXAFS calculations with the single scattering terms including the SOI in the intrinsic and extrinsic processes in order to understand the effects of the SOI on K-edge MEXAFS deeply.

2. Theory

The x-ray (linear) absorption coefficient μ with the helicity m_p $(= 0, \pm 1)$ of linearly and circularly polarized x-

rays is expanded up to the first order of relativistic corrections [6, 11]:

$$\mu(m_p) \sim \mu_{NR}(m_p) + \mu_{cross}(m_p) + \mu_{SOI}(m_p). \quad (1)$$

The non-relativistic limit μ_{NR} is written as

$$\mu_{NR}(m_p) = -2\mathrm{Im}\,\langle\varphi_c|\, d^*_{m_p} G\, d_{m_p}\,|\varphi_c\rangle\,, \quad (2)$$

$$d_{m_p}(\vec{r}) = rY_{1,m_p}(\hat{r}), \quad (3)$$

where G is the one-electron Green's function, d the dipole photon-electron excitation operator, $Y_{l,m}$ the spherical harmonics with the azimuthal quantum number l and magnetic quantum number m, and φ_c the core wavefunction. For the K-edge absorption, φ_c corresponds to the core 1s orbital. Although the cross term μ_{cross} involves in one of the relativistic effects only at the absorbing atom and has a non-negligible contribution to XMCD and MEXAFS, we do not focus on this term because the SOI is not included in it. The x-ray absorption coefficient μ_{SOI} arising from SOI is written as

$$\mu_{SOI}(m_p) = -2\mathrm{Im}\,\langle\varphi_c|\, d^*_{m_p} G\,\delta V\, G\, d_{m_p}\,|\varphi_c\rangle\,, \quad (4)$$

$$\delta V(\vec{r}) = \sum_\alpha \xi^\alpha(r_\alpha)\left(\hat{\sigma}\cdot\hat{L}^\alpha\right) \quad \left(\vec{r}_\alpha = \vec{r} - \vec{R}_\alpha\right), \quad (5)$$

$$\xi^\alpha(r) = \frac{1}{4c^2}\frac{1}{r}\frac{dv^\alpha(r)}{dr} \quad (6)$$

where δV is the SOI potential, $\hat{\sigma}$ the Pauli matrices and $\hat{L}$ the angular momentum operator. The position vector $\vec{R}$ and effective site potential v are specified by the atomic site index α. We assume that v is a spherical potential which has no overlap with other site potentials (e.g. the muffin-tin potential within the muffin-tin approximation). It should be noted that, as long as the approximation by the first order of the relativistic corrections is adopted, the SOI is taken into account as the first order perturbation. The validity of the perturbative SOI may have not been proven directly; however, the calculated results of XMCD and MEXAFS with the perturbation method show good agreement with observed spectra in literatures [7, 8, 9]. In addition, the spin-flip scattering requires the second order perturbation, which is expected to give a negligible contribution. Thus, we believe that the perturbation does not cause a fatal error for calculations of MEXAFS spectra.

Here, we restrict each term for K-edge MEXAFS to the single scattering. By using a multiple-scattering expansion up to a single scattering, G is approximated by

$$G \sim G_{\alpha_1} + G_{\alpha_1} v^{\alpha_2} G_{\alpha_2}(1-\delta_{\alpha_1\alpha_2}) + {\sum_{\alpha_3}}' G_{\alpha_1} t^{\alpha_3} G_{\alpha_2}, \quad (7)$$

$$t^\alpha = v^\alpha + v^\alpha\, G_0\, t^\alpha, \quad (8)$$

where G_0 is the free one-electron Green's function and δ_{ij} the Kronecker delta. The summation of α_3 does not include α_1 and α_2. The photoelectron scattering is not directly described by v but by the site T matrix t. The local one-electron Green's function G_α is defined by

$$G_\alpha \equiv G_0 + G_0 v^\alpha G_\alpha, \quad (9)$$

$$G_\alpha(\vec{r}\in\Omega_\alpha, \vec{r'}\in\Omega_\alpha\,;\varepsilon) = -2ik\sum_L \phi^\alpha_l(kr_{\alpha,<})Y_L(\hat{r}_\alpha)\bar{\phi}^\alpha_l(kr_{\alpha,>})Y^*_L(\hat{r}'_\alpha) \quad (r_< \equiv \min(r,r'),\quad r_> \equiv \max(r,r')\,), \quad (10)$$

$$G_{\alpha_1}(\vec{r}\in\Omega_{\alpha_1}, \vec{r'}\in\Omega_{\alpha_2(\neq\alpha_1)}\,;\varepsilon) = 2\sum_{L,L'}\tilde{G}^{\alpha_1,\alpha_2}_{L,L'}\phi_l(kr_{\alpha_1})Y_L(\hat{r}_{\alpha_1})j_l(kr'_{\alpha_2})Y^*_L(\hat{r}'_{\alpha_2}), \quad (11)$$

where Ω_α is the region belonging to α and the wavenumber $k = \sqrt{2\varepsilon}$ in the Hartree atomic unit. The photoelectron energy ε is measured from the threshold of the continuum state (e.g. the muffin-tin zero). The angular momentum index L is a short-hand notation for (l,m). The free electron propagator $\tilde{G}^{\alpha_1,\alpha_2}_{L_1,L_2}$, which is called the KKR structure constant, describes that a free electron moves from α_1 site with L_1 to α_2 site with L_2 and vice versa. The radial parts ϕ and $\bar{\phi}$ of the regular and irregular wavefunctions are defined with the radial Schrödinger equation in the Hartree atomic unit, respectively.

$$\left(-\frac{1}{2}\frac{d^2}{dr^2} + \frac{l(l+1)}{2r^2} + v^\alpha(r)\right) r f^\alpha_l(r) = \varepsilon\, r f^\alpha_l(r), \quad (12)$$

where f is ϕ or $\bar{\phi}$. For the free electron case ($v^\alpha = 0$), $\phi_l(r)$ is equal to $j_l(kr)$, where j is the spherical Bessel function. The regular wavefunction ϕ converges at $r \to 0$, whereas the irregular one $\bar{\phi}$ has a singularity at a site center.

For comparison of MEXAFS spectra to those of EXAFS, the single scattering term $\mu^{(1)}_{NR}$ of μ_{NR} is written as

$$\mu^{(1)}_{NR}(m_p) \propto -2\mathrm{Im}\sum_\sigma (\rho^\sigma)^2\,\mathcal{T}^\sigma_{m_p}, \quad (13)$$

$$\mathcal{T}^\sigma_{m_p} = 2\sum_{\alpha(\neq A)}\sum_L \tilde{G}^{A,\alpha}_{1m_p,L}\, t^{\alpha,\sigma}_l\, \tilde{G}^{\alpha,A}_{L,1m_p}, \quad (14)$$

$$\rho^\sigma = \frac{1}{\sqrt{4\pi}}\int r^3\varphi^\sigma_c(r)\phi^{A,\sigma}_1(r)\,dr, \quad (15)$$

where σ $(=\pm)$ is the spin index and A the site index of the absorbing atom.

We decompose the SOI term μ_{SOI} by $\mu_{SOI,in}$ and $\mu_{SOI,ex}$. The intrinsic term $\mu_{SOI,in}$ includes the SOI at the absorbing atom in a radial integral but not in the scattering process. The single scattering term $\mu^{(1)}_{SOI,in}$ of $\mu_{SOI,in}$ is written as

$$\mu^{(1)}_{SOI,in}(m_p) \propto 2\left(-2\mathrm{Im}\sum_\sigma \rho^\sigma\delta\rho^\sigma\mathcal{T}'^\sigma_{m_p}\right), \quad (16)$$

$$\mathcal{T}'^\sigma_{m_p} = m_p\sigma\mathcal{T}^\sigma_{m_p}, \quad (17)$$

$$\delta\rho = \frac{-2ik}{\sqrt{4\pi}}\int r^2\, r'^3\phi^A_1(r)\,\xi^A(r) \times \phi^A_1(r_<)\,\bar{\phi}^A_1(r_>)\,\varphi_c(r')\,dr\,dr'. \quad (18)$$

While the extrinsic term $\mu_{SOI,ex}$ includes the SOI at all atomic sites in the scattering processes. Since single scattering processes do not have a scattering at the absorbing atom, the single scattering term $\mu^{(1)}_{SOI,ex}$ has the contribution of the SOI at the surrounding atoms.

$$\mu^{(1)}_{SOI,ex}(m_p) \propto -2\mathrm{Im}\sum_{\sigma}(\rho^{\sigma})^2\,\Xi^{(1),\sigma}_{m_p}, \tag{19}$$

$$\Xi^{(1),\sigma}_{m_p} = 4\sum_{L} m\sigma \sum_{\alpha(\neq A)} \tilde{G}^{A,\alpha}_{1m_p,L}\left[\xi^{(1)}\right]^{\alpha,\sigma}_{l}\tilde{G}^{\alpha,A}_{L,1m_p}, \tag{20}$$

$$\left[\xi^{(1)}\right] = [\xi]^{j,j} - 4ik\,[\xi v]^{j,j} - 4k^2\,[v\xi v]^{j,j}\,, \tag{21}$$

The radial integrals are defined by

$$[\xi]^{f_1,f_2} = \int r^2\, f_1(r)\,\xi(r)\,f_2(r)\,dr, \tag{22}$$

$$[\xi v]^{f_1,f_2} = [v\xi]^{f_2,f_1} = \int r^2\, r'^2\, f_1(r)\,\xi(r)\phi(r_<)\,\bar{\phi}(r_>)\,v(r')\,f_2(r')\,dr\,dr', \tag{23}$$

$$[v\xi v]^{f_1,f_2} = \int r^2\, r'^2\, r''^2\, f_1(r)\,v(r)\,\phi(r_<)\,\bar{\phi}(r_>) \times \xi(r')\,\phi(r'_<)\,\bar{\phi}(r'_>)\,v(r'')\,f_2(r'')\,dr\,dr'\,dr'' \quad (\,r'_< \equiv \min(r',r''),\quad r'_> \equiv \max(r',r'')\,), \tag{24}$$

where the functions f_1 and f_2 are the spherical Bessel function j and/or the regular solution ϕ. Although we have reported in Ref. 11 that the third term $[v\xi v]^{j,j}$ in $\left[\xi^{(1)}\right]$ makes $\Xi^{(1)}$ non negligible for XMCD [11], this has not been checked for MEXAFS. Therefore, we check the contribution of our present $\Xi^{(1)}$ to MEXAFS in the next section.

Besides, according to Brouder's method [8, 9], $\Xi^{(1)}$ may be approximated by the following $\Xi'^{(1)}$

$$\Xi'^{(1),\sigma}_{m_p} = 4\sum_{L} m\sigma \sum_{\alpha(\neq A)} \tilde{G}^{A,\alpha}_{1m_p,L}\left[\xi^{(\infty)}\right]^{\alpha,\sigma}_{l}\tilde{G}^{\alpha,A}_{L,1m_p}, \tag{25}$$

$$\left[\xi^{(\infty)}\right] = [\xi]^{\phi,\phi}. \tag{26}$$

The radial integral $\left[\xi^{(\infty)}\right]$ originates from the full MS term $\Xi^{(\infty)}$ [11] which does not have the same expression as the single scattering terms $\Xi^{(1)}$ and $\Xi'^{(1)}$. We also discuss the difference between $\Xi^{(1)}$ and $\Xi'^{(1)}$.

3. Results and Discussion

EXAFS oscillations $\chi(m_p)$ for each m_p is obtained by dividing of a single scattering term $\mu^{(1)}(m_p)$ by the atomic absorption term $\mu^{(0)}_{NR}$ which has no scattering factor.

$$\chi(m_p) = \mu^{(1)}(m_p)\,/\,\mu^{(0)}_{NR}(m_p). \tag{27}$$

Hence, EXAFS and MEXAFS spectra (χ and $\Delta\chi$) are defined by

$$\chi = \chi(0), \tag{28}$$

$$\Delta\chi = \chi(+;B-) - \chi(-;B-), \tag{29}$$

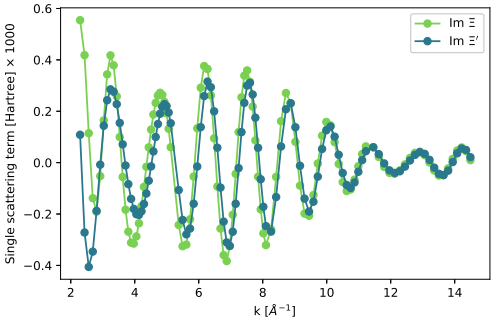

Figure 1: Compraison between the imaginary parts of the single scattering terms of Ξ and Ξ'.

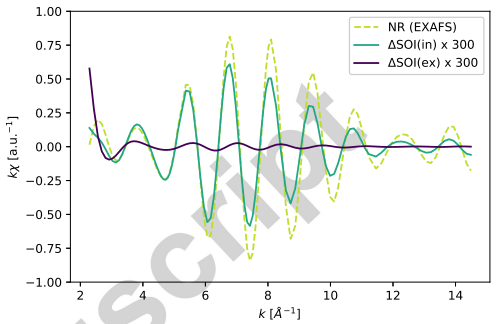

Figure 2: Contributions of each term to MEXAFS oscillations. The calculated EXAFS oscillations are also shown for comparison.

where $B-$ indicates that the magnetic field is antiparallel to the incident x-ray direction. In order to perform a numerical check, we employ BCC iron as a reference system for MEXAFS. Although a dynamical potential plays an important role to reproduce observed EXAFS and MEXAFS spectra, a static potential is sufficient for the check because we use the same potential for each $\mu^{(1)}$ term and only concentrate to relationship between the terms. The spin-polarized static potential is obtained by use of the LMTO band structure code [12]. Moreover, the structural model cluster includes up to the second shell of neighbours for simplicity.

Figure 1 shows a good agreement between $\Xi^{(1)}$ and $\Xi'^{(1)}$ for $\mu_{SOI,ex}$ in the higher k region ($k > 4$). This indicates that the approximation using $\Xi'^{(1)}$ is expected to be a good approximation for MEXAFS because the MEXAFS analysis use the spectra beyond $k \sim 4$ in order to avoid the contribution of multi-electron excitation [1]. This result also demonstrate the advantage of the approximation for the numerical calculation because the calculation of $[\xi]^{\phi,\phi}$ is much faster than that of $[v\xi v]^{j,j}$, which includes a triple integral with singular points as shown in eq. (24). In the XMCD k region ($k < 4$), the difference becomes large, which is consistent with the previous XMCD study [11].

Figure 2 shows the comparison between $\Delta\chi_{SOI,in}$ and $\Delta\chi_{SOI,ex}$ as well as EXAFS oscillations χ. Our calcu-

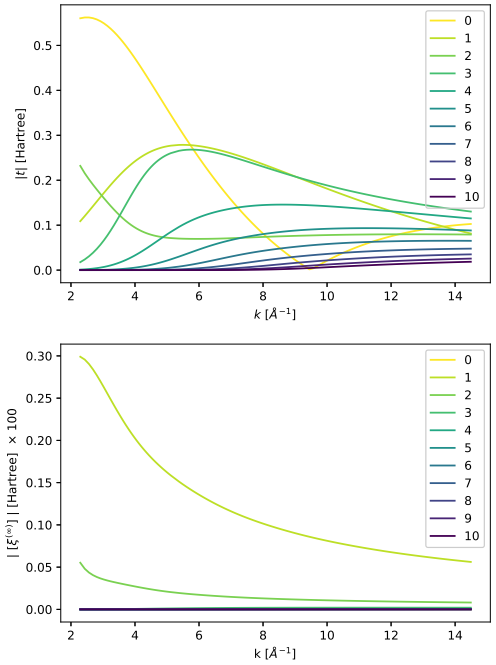

Figure 3: Absolute values of the partial wave components of t and $\left[\xi^{(\infty)}\right]$. Note that the component of $\left[\xi^{(\infty)}\right]$ with $l = 0$ is zero because $m = 0$.

lated intensity of $\Delta\chi_{SOI,ex}$ is about 10 times smaller than that of $\Delta\chi_{SOI,in}$. A previous result in Ref. 5 showed that $\Delta\chi_{SOI,ex}$ using only $[\xi]^{j,j}$ is a thousand times smaller than $\Delta\chi_{SOI,in}$ [5]. Hence, although the present derivation scales the calculated result by the factor of 100, $\mu^{(1)}_{SOI,ex}$ still does not exhibit any dominant contribution to MEXAFS. This result is independent on the cancellation of various MS contributions in the extrinsic process shown by the full MS calculations [9]. Therefore, we conclude that the mechanism of the negligible SOI contribution based on the cancellation is not supported at least within the single-scattering approximation. This is different from the case of XMCD, where $\mu^{(1)}_{SOI,ex}$ leads to a non-negligible contribution [11].

Figure 3 shows the partial wave components of t and $\left[\xi^{(\infty)}\right]$ in order to understand why $\Delta\chi_{SOI,ex}$ is rather small despite the substantial contribution of $\Xi^{(1)}$ to XMCD [11]. The partial wave components of $\left[\xi^{(\infty)}\right]$ decrease very rapidly with l in all k range. On the other hand, the partial wave components of t decrease more slowly. In addition, the higher partial wave components increase in the higher k region. This difference can be understood by the effective range of the site potential and SOI. Generally, higher partial wave components describe the original term in the outer range region because of the stronger centrifugal force. Since the radial component $\xi(r)$ of SOI is defined by the gradient of the site potential as shown in eq. (6), the effective range of $\xi(r)$ is essentially limited just around the nuclei. This explains why only a small number of the partial wave components of SOI is effective. Moreover, the maximum partial wave l_{max} at a k point is given by $l_{max} \leq kR_{atom}$, where R_{atom} is the radius of the potential of an atomic sphere. Therefore, the larger k, the lesser the contribution of the largest partial wave component of $[\xi]$ to MEXAFS.

4. Conclusion

We have demonstrated an effect of the SOI within the photoelectron single scattering theory for K-edge MEXAFS. The present derivation scales MEXAFS oscillations in the extrinsic process by the factor of 100. Brouder's approximation gives a good agreement within the present derivation in the k region for MEXAFS, and reduces the computational cost. However, in spite of the scaling, the single scattering term of the SOI at surrounding atomic sites has still a negligible contribution to MEXAFS. This small contribution partially comes from the extremely narrow effective range of the SOI and from the small number of its effective partial wave components. This small number of the partial wave components leads to faster computations of MS terms including the scattering-site SOI for MEXAFS.

References

[1] Nakamura, T., Mizumaki, M., Watanabe, Y., Nanao, S., 1998. Distribution of Spin Polarization in Ferrimagnetic $DyFe_2$ by a Novel Analysis of Magnetic EXAFS. J. Phys. Soc. Jpn. 67, 3964.

[2] Ebert, H., Popescu, V., Ahlers, D., 1999. Fully relativistic theory for magnetic EXAFS: Formalism and applications. Phys. Rev. B 60, 7156.

[3] Ankudinov, A.L., Rehr, J.J., 1995. Calculation of x-ray magnetic circular dichroism in Gd. Phys. Rev. B 52, 10214.

[4] Ankudinov, A.L., Rehr, J.J., 1997. Relativistic calculations of spin-dependent x-ray-absorption spectra. Phys. Rev. B 56, R1712.

[5] Fujikawa, T., Nagamatsu, S., 2002. Multiple Scattering Approach to the Theory of Angular Dependence of K-edge X-Ray Magnetic Circular Dichroism. Jpn. J. Appl. Phys. 41, 55.

[6] Fujikawa, T., Nagamatsu, S., 2003. Relativistic multiple scattering theory of K-edge X-ray magnetic circular dichroism. J. Electron Spectrosc. Relat. Phenom. 129, 55.

[7] Brouder, Ch., Hikam, M., 1991. Multiple-scattering theory of magnetic x-ray circular dichroism. Phys. Rev. B 43, 7334.

[8] Brouder, Ch., Alouani, M., Bennemann, K. H., Phys. Rev. B 54, 7334.

[9] Brouder, Ch., Alouani, M., Giorgetti, Ch., Dartyge, E., 1996. Multiple-Scattering Approach to Magnetic EXAFS. Spin-Orbit-Influenced Spectroscopies of Magnetic Solids (Springer, Berlin), 259-274.

[10] Wende, H., Srivastava, P.S., Arvanitis, D., Wilhelm, F., Lemke, L., Ankudinov, A., Rehr, J.J., Freeland, J.W., Idzerda, Y.U., Baberschke, K., 1999. Magnetic L-edge EXAFS of 3d elements: multiple-scattering analysis and spin dynamics. J. Synchrotron Rad. 6, 696-698.

[11] Koide, A., Niki, K., Sakai, S., Fujikawa, T., 2016. Real-space multiple-scattering theory of XMCD including spin-orbit interaction in scattering process. J. Phys.: Conf. Ser. 712, 012010.

[12] Andersen, O.K., Jepsen, O., 1984. Explicit, First-Principles Tight-Binding Theory. Phys. Rev. Lett 53, 2571